Newton's Rings Experiment

Under-Graduate Science Laboratory – BS 192 (Group - 7)

Birudugadda Srivibhav – 22110050
Vubbani Bharath Chandra – 22110293
Ankeshwar Ruthesha – 22110024
Kirtankumar Patel – 22110185

1 Objective

The objective of this experiment is to determine the radius of curvature of a plano-convex lens by using the Newton's rings method. This experiment utilizes the phenomenon of interference of light by amplitude division, where circular interference fringes (Newton's rings) are formed due to the air gap between a plano-convex lens and a flat glass surface when illuminated with monochromatic light. By analyzing the diameters of the bright and dark fringes, the radius of curvature of the lens can be accurately calculated.

2 Apparatus Description

- **Microscope**: A high-precision optical instrument used to observe the interference fringes (Newton's rings) and measure their diameters. It is equipped with an XY translation stage for fine movements in the X and Y directions.
- **Beam Splitter**: A device that reflects light at a 45° angle to direct the light towards the air gap between the lens and glass plate, while allowing the reflected light to pass through for observation.
- **Plano-Convex Lens**: A lens with one flat surface and one convex surface, which creates an air gap when placed on the optical flat. The curvature of this lens generates the interference pattern when illuminated.

- **Optical Flat**: A highly polished flat glass plate that provides a reference surface for the plano-convex lens, ensuring that the air gap formed between them is uniform for interference to occur.
- **XY Translation Stage**: A precision mechanism that allows the microscope to be moved smoothly along the X and Y axes, facilitating the accurate measurement of the ring diameters.
- **Sodium Vapor Lamp**: A light source emitting nearly monochromatic yellow light at a wavelength of 5893 Å, essential for creating well-defined interference fringes.

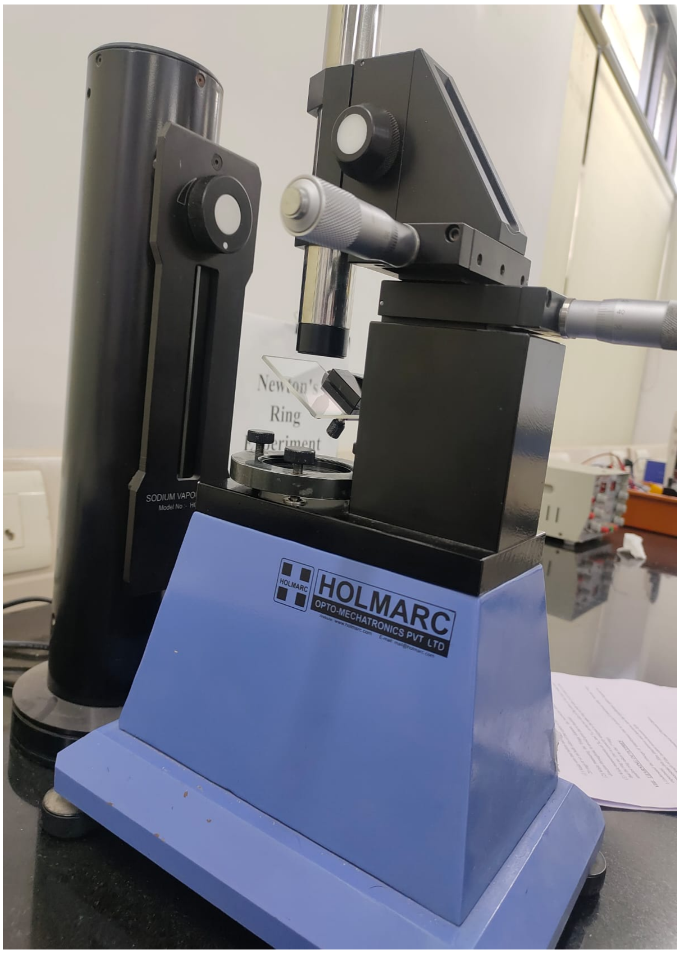

Figure 1: Apparatus for Newton's Rings experiment.

3 Theory

3.1 Historical Background[1]

Newton's rings were first observed and explained by Sir Isaac Newton in the late 17th century during his investigations into the nature of light. In his landmark work Opticks, Newton explored how light interacts with surfaces, leading to his discovery of the interference patterns now known as Newton's rings. These rings are formed when light waves reflected from the curved surface of a plano-convex lens and a flat glass plate interfere with one another, producing a series of concentric bright and dark fringes. At the time, this phenomenon provided crucial insights into the wave-like behavior of light, challenging the prevailing corpuscular theory, which treated light as particles.

The discovery of Newton's rings marked a pivotal moment in the development of wave optics and laid the groundwork for later advancements in the study of light. Over time, the experiment became a key demonstration of thin film interference and is now used widely to measure the radius of curvature of lenses with great accuracy. Newton's pioneering work on the interference of light remains fundamental to modern optics, influencing everything from the design of optical instruments to the development of new technologies in fields such as microscopy, astronomy, and materials science.

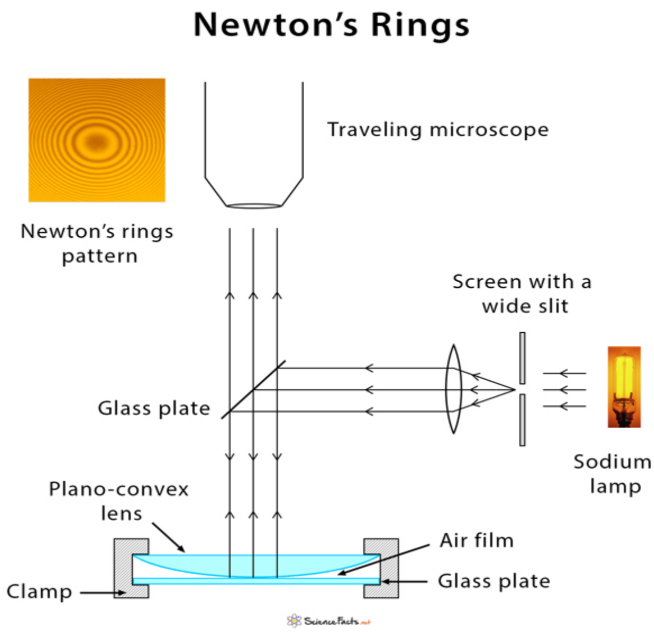

Figure 2: Illustration of Newton's Rings experiment[2].

3.2 The Newton's Rings Experiment

3.2.1 Interference Conditions

The formation of Newton's rings can be explained by analyzing the optical path difference between the two reflected rays. The interference conditions are as follows:

- **Dark fringe:**

$$2t \approx 2n\left(\frac{\lambda}{2}\right) \tag{1}$$

- **Bright fringe:**

$$2t \approx (2n+1)\left(\frac{\lambda}{2}\right) \tag{2}$$

In this case, t denotes the air gap at the specified point, n is an integer, and λ is the wavelength of the monochromatic light.

3.2.2 Derivation of the Radius and Diameter of Fringes

Referring to Figure-1 and analyzing the geometry of the lens system, the connection between the radius of the n-th bright fringe r_n and the radius of curvature R of the lower lens surface is described by:

$$R^2 = r_n^2 + (R-t)^2 \tag{3}$$

Assuming t^2 is negligible for a thin lens with minor curvature, we approximate:

$$t \approx \frac{r_n^2}{2R} \tag{4}$$

Substituting this into the interference condition for the n-th bright fringe yields:

$$r_n^2 = \frac{(2n+1)\lambda R}{2} \tag{5}$$

From this, the diameter of the n-th bright fringe can be determined as:

$$D_n^2 = 2(2n+1)\lambda R \tag{6}$$

In a similar manner, the diameter of the n-th dark fringe is expressed by:

$$D_n'^2 = 4n\lambda R \tag{7}$$

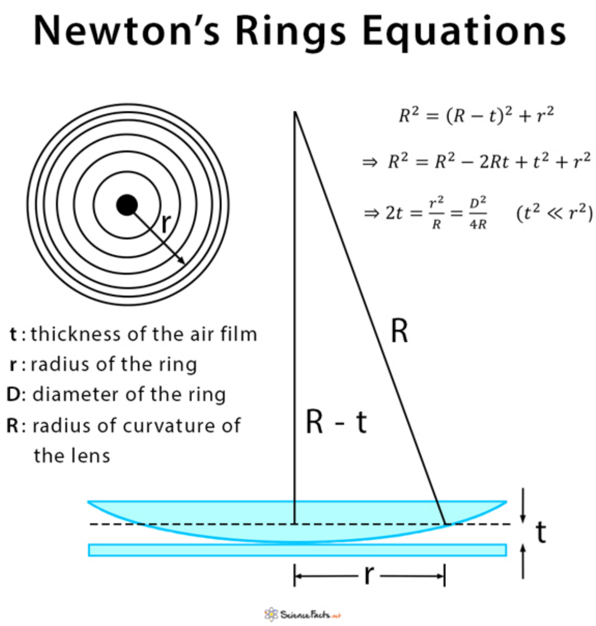

Figure 3: Schematic Diagram of Newton's Rings [2].

3.2.3 Difference in Diameters Between Fringes

Due to potential imperfections in the contact between the two lens surfaces at the center, it can be challenging to precisely determine the order of the fringes. Nevertheless, the difference in diameters between two bright (or dark) fringes of orders n_1 and n_2 can be expressed as:

$$\frac{D_{n_1}^2 - D_{n_2}^2}{n_1 - n_2} = 4\lambda R \tag{8}$$

This formula allows for the determination of the **radius of curvature** R of the lens by measuring the diameters of various fringes.

4 Procedure

4.1 Preparation and Setup

1. The optics were cleaned using isopropyl alcohol.
2. The optically flat disc was placed near the microscope objective.
3. The plano-convex lens was positioned on top of the flat disc with only a point of contact.

4. The beam splitter was inserted into its holder and secured with screws.
5. The sodium vapor lamp was turned on and allowed to reach its full intensity.
6. The lamp was placed in front of the microscope, and the beam splitter was adjusted to a 45° angle.
7. The image was focused by adjusting the distance of the microscope tube.
8. The crosswire was aligned with the direction of the travelling microscope.

4.2 Alignment of the Crosswire

1. With the fringe pattern visible, the crosswire was aligned with the center of the pattern using micrometer screws.
2. The movement of the micrometer caused a shift in the ring pattern, which was observed.

4.3 Microscope Positioning

1. The microscope was positioned such that one crosswire made tangential contact with the rings.
2. The setup allowed traversal through 20 rings by rotating the micrometer screw in one direction.

4.4 Measurement of Dark Fringes

1. The crosswire was moved to a prominent dark ring (designated as the m-th ring).
2. The crosswire was centered on the ring's width, and its position (X_m) was recorded.
3. The crosswire was then moved towards the center, aligning it with alternate dark rings, and positions were noted (X_{m-1}, X_{m-2}, ..., X_2, X_1).
4. After crossing the center, the crosswire was positioned at diametrically opposite points, and these positions were recorded (X'_1, X'_2, X'_3, ..., X'_{m-2}, X'_{m-1}).

4.5 Calculations

1. The ring number $(1, 2, \ldots, m)$, X_m, X'_m, ring diameter D_m $(= X_m - X'_m)$, and D_m^2 were tabulated.

2. D_m^2 (Y-axis) versus m (X-axis) was plotted using Python. The slope S was calculated as
$$S = \frac{D_m^2 - D_{m-2}^2}{m - (m-2)}$$
The radius of curvature R was then determined using equation (8). The wavelength λ used was 5893 Å.

3. We calculated the error in measurement using various methods discussed in the following sections

Ring Number	$\mathbf{X_m}$ (in mm)	$\mathbf{X'}_m$ (in mm)	Diameter (in mm)	Diameter squared (in mm^2)
1	11.26	9.93	1.33	1.7689
2	11.46	9.68	1.78	3.1684
3	11.62	9.51	2.11	4.4521
4	11.76	9.36	2.40	5.7600
5	11.90	9.23	2.67	7.1289
6	12.02	9.13	2.89	8.3521
7	12.13	9.03	3.10	9.6100
8	12.23	8.92	3.31	10.9561
9	12.31	8.84	3.47	12.0409
10	12.40	8.75	3.65	13.3225
11	12.49	8.66	3.83	14.6689
12	12.57	8.59	3.98	15.8404
13	12.65	8.51	4.14	17.1396
14	12.71	8.45	4.26	18.1476
15	12.78	8.37	4.41	19.4481
16	12.84	8.30	4.54	20.6116
17	12.91	8.24	4.67	21.8089
18	12.98	8.17	4.81	23.1363
19	13.04	8.12	4.92	24.2064
20	13.07	8.05	5.02	25.2004

Table 1: Measurements of positions of diametrically opposite points on the circular fringes.

5 Results and Discussion

5.1 Linear Regression Analysis

The data from Table 1 was used to plot D_m^2 (the square of the diameter) against the ring number m. The plot, illustrated in Figure 4, displayed a linear trend, which aligns with the theoretical expectation.

To analyze the data further, we performed a linear regression analysis in Python. The slope of the regression line was then used to calculate the radius of curvature R as per equation (8). The analysis yielded a **slope of** 1.2356 **mm**^{2}. With this slope and using the wavelength $\lambda = 5893\,\text{Å}$, the radius of curvature R was found to be **524.17 mm**.

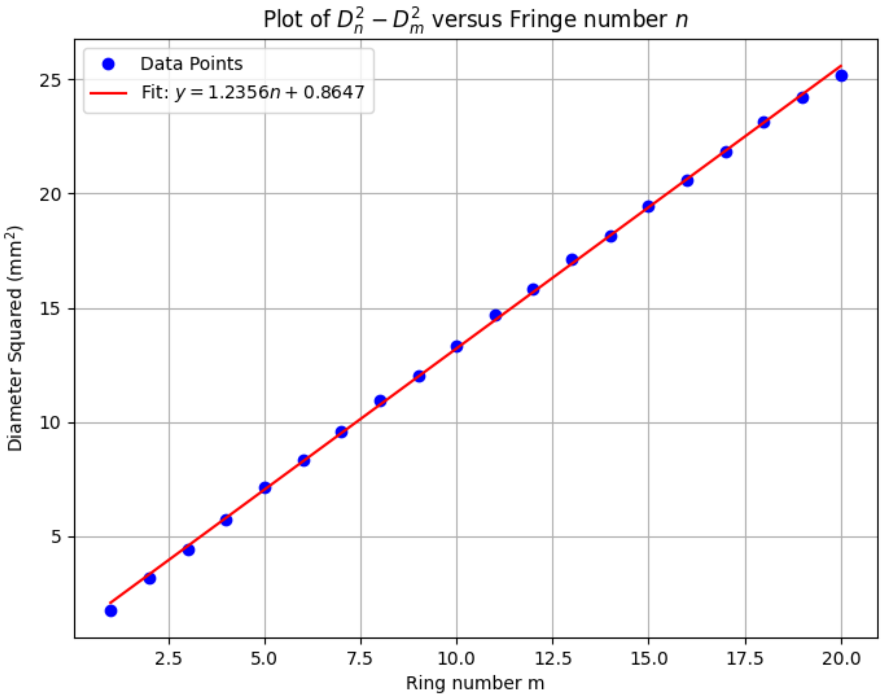

Figure 4: Graph of D_m^2 versus Ring Number m.

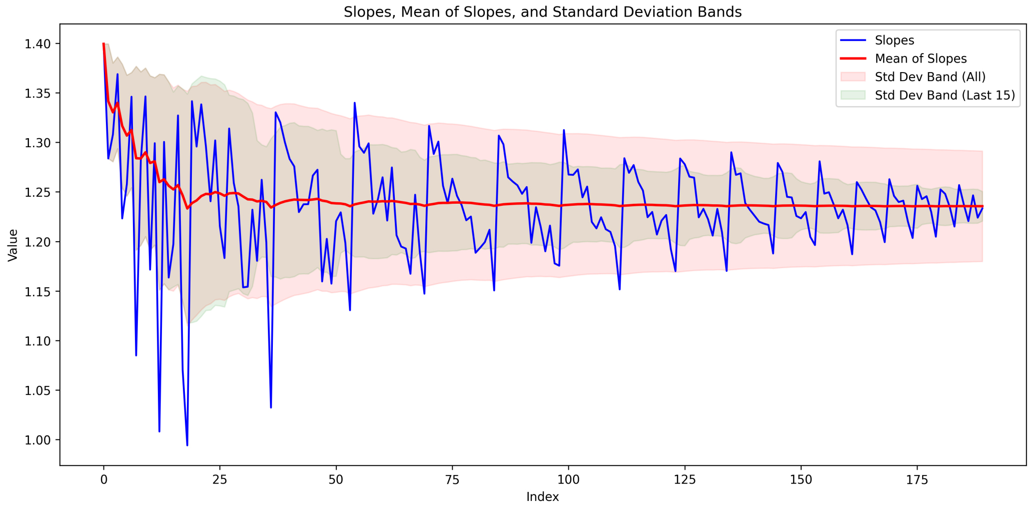

Figure 5: Variation in slope values with different pairs of data points.

5.2 Probabilistic Analysis

To account for variations in slope values, we conducted a *probabilistic analysis*. During the experiment, 20 data points were collected, and we computed the slopes for all possible pairs of points, resulting in 190 slope values. This approach allowed us to examine the behavior of the slopes more comprehensively, rather than relying on a single linear fit.

The variability in these slopes was analyzed by calculating the *mean and standard deviation*, providing insights into the distribution of slope values across different point pairs. This analysis helped us understand the robustness of the calculated slope and its sensitivity to the selection of points.

A histogram of the slope values was plotted (Figure 6), which showed that slope values tend to *converge* as the distance between points increases. This indicates that pairs of points that are farther apart yield more consistent slope estimates, likely because short-range fluctuations are minimized over larger intervals. The histogram also helped identify any potential outliers or anomalies in the slope distribution.

Using the probabilistic approach, the mean radius of curvature was calculated to be $\overline{R} = 52.416\,\text{cm}$, with a *standard deviation* of $\sigma = 2.365\,\text{cm}$. This provides a reliable estimate of the radius while accounting for the inherent variability in the data. The relatively small standard deviation suggests that the slope values are closely clustered around the mean, confirming the precision of the results.

Figure 5 illustrates the variation of slope between any two points, providing a detailed view of the fluctuations in slope as a function of point separation. This figure complements Figure 4, which shows the relationship between the measured diameters and the ring number, further solidifying the overall analysis.

Together, these figures and statistical measures provide a comprehensive understanding of the data, highlighting both the central trends and the variability in slope estimates.

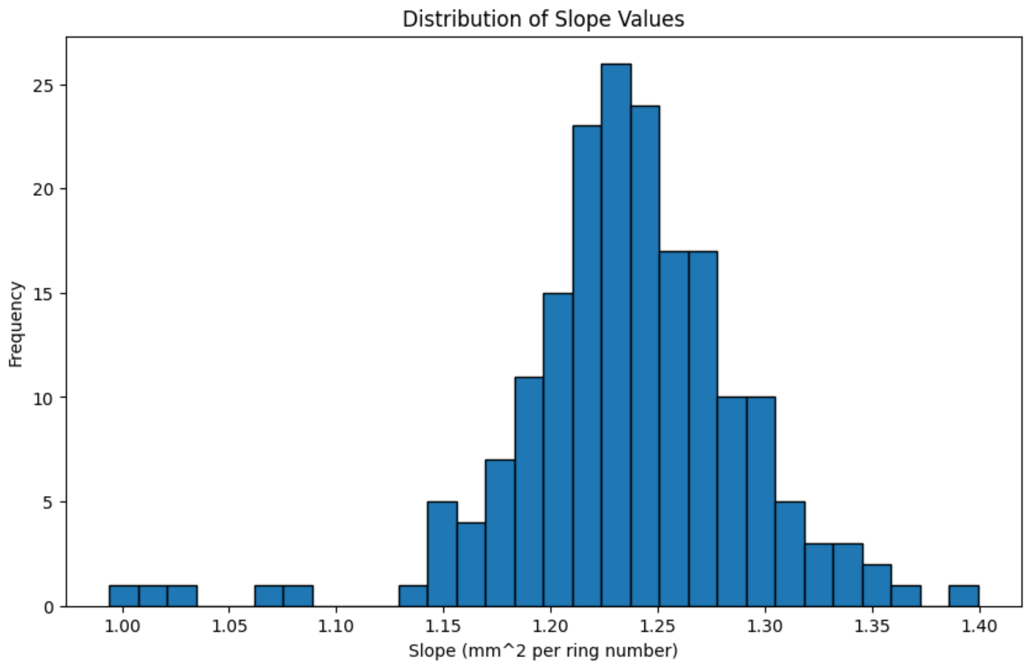

Figure 6: Histogram of the slope values calculated from different point pairs.

5.3 Differential Method Analysis

The precision of measuring the position of the circular fringes was 0.01 mm, which translated to a precision of 0.02 mm for the diameter of the fringes. The precision in the squared diameter was determined as:

$$\Delta(D^2) = 2D \cdot \Delta(D) = 0.04D$$

By applying logarithmic differentiation to the relationship between the squared diameter and the radius of curvature, we derived the following equation for the precision of R:

$$\frac{\Delta(D_n^2) - \Delta(D_m^2)}{D_n^2 - D_m^2} = \frac{\Delta R}{R}$$

Using the above equation, we get:

$$\frac{0.04}{D_n + D_m} = \frac{\Delta R}{R}$$

To find the maximum precision of R, denoted as ΔR, we use the maximum value of R (59.371 cm) and the minimum value of $(D_n + D_m)$ (3.11 mm) from our measurements:

$$\frac{0.04}{1.33 + 1.78} = \frac{\Delta R}{59.371}$$

$$\Delta R = \frac{59.371 \times 0.04}{3.11} \approx 7.64\,\text{mm}$$

We present the final result as $R = \text{R}_{\text{mean}} \pm 0.764\,\text{cm}$, with the mean radius being 52.416 cm from the previous analysis.

Therefore, the final value for the radius of curvature is:

$$R = 52.416\,\text{cm} \pm 0.764\,\text{cm}$$

6 Potential Sources of Error

Despite obtaining reliable results, a few factors might have led to minor discrepancies in the final measurements:

- **Instrumental Inaccuracies:** Slight imprecision in measuring the ring diameters or improper calibration of the tools might have influenced the outcome.
- **Environmental Factors:** Fluctuations in room temperature or air movement could alter the refractive index, causing minor changes in the fringe pattern.
- **Lens Misalignment:** Any minor misalignment between the plano-convex lens and the flat glass surface might distort the observed ring pattern.

- **Human Error:** Variations in identifying the precise fringe boundaries could introduce some inconsistencies in the results.
- **Optical Imperfections:** Defects or imperfections in the plano-convex lens may result in deviations from the expected ring pattern, affecting overall accuracy.

7 Answer to the Questions

1. Why are the interference rings circular in shape? [3]

In Newton's ring experiment, the circular interference rings arise due to the symmetrical arrangement of the setup. A plano-convex lens placed on a flat glass surface creates a thin air film, whose thickness gradually increases outward from the point of contact. Since the thickness remains uniform at any given distance from the contact point, light waves reflecting off the surfaces interact consistently along circular paths, leading to the formation of circular rings. The circular shape of the air film's thickness is the primary reason for the round interference patterns.

2. Why do the rings get closer as order of the rings increases? [4]

The size of bright rings increases according to the formula

$$D_n^2 = 2\lambda R(2n+1),$$

and for dark rings, the formula is

$$D_n^2 = 4n\lambda R.$$

Both formulas show that the ring diameter grows with increasing order, but at a decreasing rate. As you move to higher-order rings (such as the tenth or twentieth), the difference in size between consecutive rings reduces. This explains why the rings appear closer together as their order increases.

3. What would be the effect of using white light instead of monochromatic light? [5]

White light contains multiple wavelengths corresponding to different colors, ranging from red to violet. Since each wavelength produces its own set of interference rings, overlapping patterns from different colors emerge. This leads to a multicolored fringe pattern, with each ring displaying a spectrum of colors.

4. What would be the shape of the rings if a wedge-shaped prism is kept inverted on the glass plate? [6]

If a wedge-shaped prism is inverted on a glass plate in place of the plano-convex lens, the circular interference rings would transform into a pattern of curved fringes. This happens because the wedge creates a linearly varying air film thickness, unlike the uniform radial thickness of the lens. Consequently, the interference pattern changes to a series of parallel or slightly curved lines instead of circular rings.

Conclusion

In this experiment, the primary goal was to measure the radius of curvature of a lens using Newton's Rings. The formation of circular interference fringes occurs due to the air gap between the plano-convex lens and the glass plate, producing concentric dark and bright rings. A central dark ring is observed, attributed to the radial symmetry of the air gap at the contact point. As the distance from the central fringe increases, the fringe width decreases while the brightness intensifies. These patterns arise from the constructive and destructive interference of light.

The radius of curvature determined was:

$$R = 52.416\,\text{cm} \pm 0.764\,\text{cm}$$

The standard deviation is found to be 2.365 cm. This deviation can be attributed to potential imperfections on the glass surface, measurement inaccuracies in X_m and X'_m, and temperature fluctuations that may influence the dimensions of the optical components, thereby affecting the interference pattern observed.

8 Author Contributions

- **Birudugadda Srivibhav**
  - Collected and recorded the experimental data.
  - Created and formatted the tables and figures used in the report.
  - Compiled the results and discussion sections, including interpreting the data and doing the error analysis.

- **Vubbani Bharath Chandra**
  - Collected and recorded the experimental data.
  - Formatted and finalized the report.
- **Ankeshwar Ruthesha**
  - Collected and recorded the experimental data.
  - Drafted the conclusion section, addressing the accuracy of the experimental results and potential sources of error.
- **Kirtankumar Patel**
  - Generated plots using Python based on the experimental data.

9 References

1 R. Chandrasekharan, "Isaac Newton: Facts, Quotes Contributions," Live Science, https://www.livescience.com. [Accessed: 06-Sep-2024].

2 Science Facts, "Newtons Rings," https://www.sciencefacts.net/newtons-rings.html. [Accessed: Sep 6, 2024].

3 "Why do Newton Rings Form in Circular Patterns?" Physics Forums, 23 Mar. 2010, https://www.physicsforums.com/. [Accessed: Sep 6, 2024].

4 "Newton's Ring Experiment." 101Viva, 17 Feb. 2015, https://101viva.wordpress.com/2015/02/17/newtons-ring-experiment/. [Accessed: Sep 6, 2024].

5 Byju's. (n.d.). Why monochromatic light is used in Newton's ring? Retrieved September 6, 2024, from https://byjus.com/question-answer/why-monochromatic-light-is-used-in-newtons-ring/.

6 Answer2Questn. (2013, March). Newton's rings Q7. Retrieved September 6, 2024, from https://answer2questn.blogspot.com/2013/03/newtons-rings-q7.html

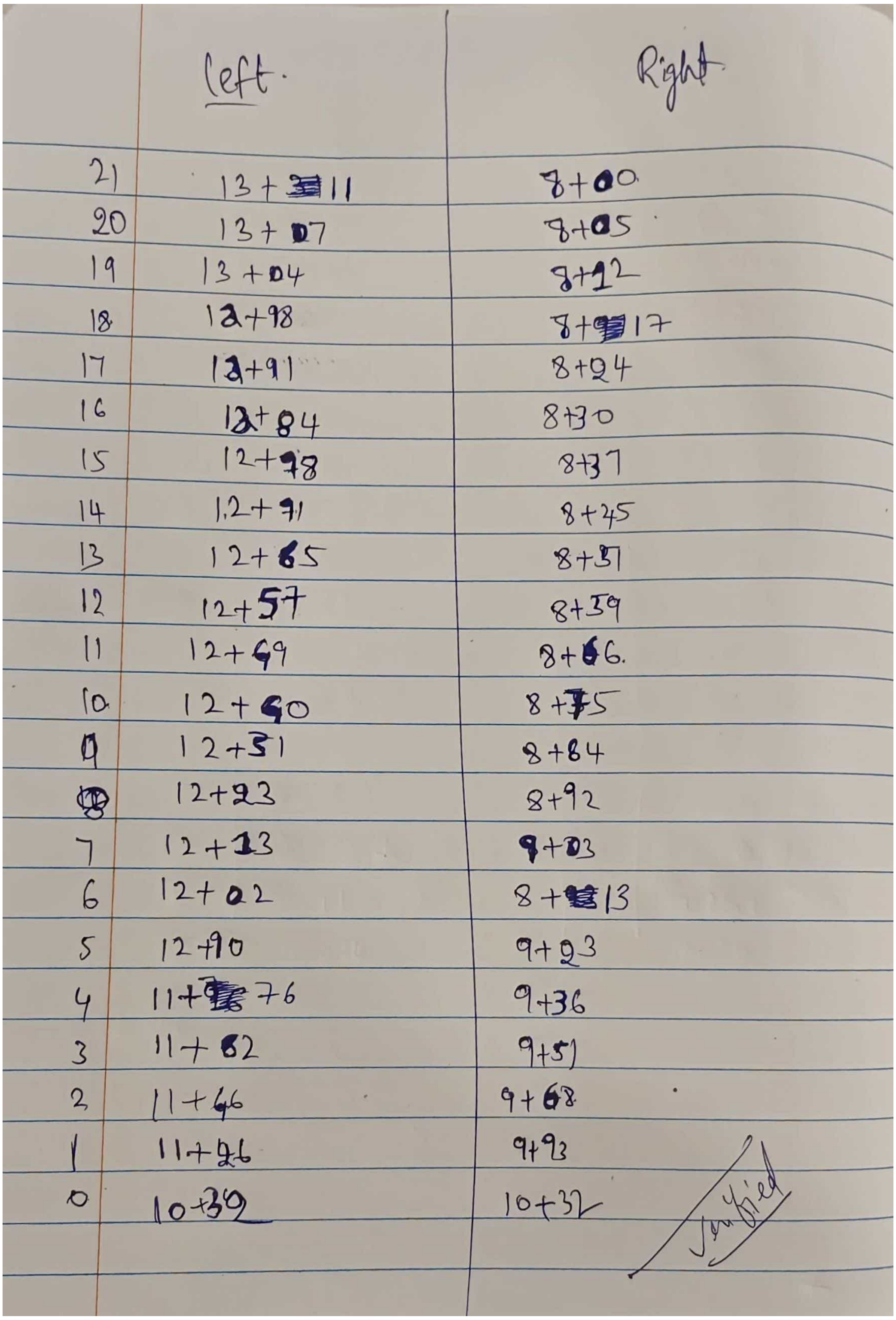

	Left	Right
21	13+11	8+00
20	13+07	8+05
19	13+04	8+12
18	12+98	8+17
17	12+91	8+24
16	12+84	8+30
15	12+78	8+37
14	12+71	8+45
13	12+65	8+51
12	12+57	8+59
11	12+49	8+66
10	12+40	8+75
9	12+31	8+84
8	12+23	8+92
7	12+13	9+03
6	12+02	8+13
5	12+90	9+23
4	11+76	9+36
3	11+62	9+51
2	11+46	9+68
1	11+26	9+93
0	10+32	10+32

Verified

Figure 7: Lab Recordings